

STUDIES OF COUPLED-BUNCH INSTABILITY IN THE HL-LHC*

C. C. Becker^{†1}, R. Calaga, B. E. Karlsen-Baeck, I. Karpov, H. Timko
CERN, Geneva, Switzerland

¹also at TU Wien, Vienna, Austria

Abstract

Beam dynamics studies, and in particular detailed macroparticle simulations, are challenging for high-energy hadron synchrotrons due to the large number of circulating bunches. The High-Luminosity Large Hadron Collider (HL-LHC) will accelerate beams with about twice the initial LHC design intensity. It will also feature additional installations such as the crab cavities, which increase the total impedance of the accelerator. In the longitudinal plane, the baseline HL-LHC scenario will push the beam parameters close to the stability limit. It is therefore of interest to study the impact of the crab cavity higher-order-mode impedances, which could lead to coupled-bunch instabilities (CBI), on the beam stability. This is particularly important in the presence of a broad-band impedance, which was predicted to lower the CBI threshold. In this contribution, particle-tracking simulation setups for instabilities, driven by either broad- or narrow-band impedances, are investigated. This paves the way for CBI simulations that take into account both impedance sources, to study the longitudinal stability limits at injection.

INTRODUCTION

Both narrow-band (NB) as well as broad-band (BB) impedances, or equivalently, long-range and short-range wake fields, can drive beam instabilities in accelerators. NB impedances arise typically from resonant modes in cavity-like structures and can drive coupled-bunch instabilities (CBI). BB impedances originate, for instance, from geometric discontinuities, resistive-wall effects, or non-ideal devices within the accelerator and are responsible for single-bunch effects such as the loss of Landau damping (LLD). In previous theoretical work [1], it was shown that the longitudinal thresholds for CBI and LLD are closely linked and that, especially when operating close to the LLD threshold, the BB impedance can reduce the CBI threshold. As part of the upgrade to HL-LHC, crab cavities are going to be installed to help increase the luminosity. Their higher-order modes (HOM) potentially drive CBI and thereby limit the performance [2]. The beam parameters after the upgrade are expected to be close to the LLD threshold. Consequently, to accurately investigate the longitudinal beam stability, both impedance sources must be considered.

To predict the behaviour of the beam after injection into the LHC, macroparticle simulations with the BLoND [3] simulation suite are performed. However, the macroparticle analysis of BB and HOM effects each come with their

challenges. Whilst the analysis of single-bunch LLD requires high time resolution, and thereby a large number of macroparticles per bunch, CBI studies require the tracking of hundreds of bunches. This work examines the macroparticle simulation requirements associated with LLD, and CBI induced by the crab-cavity HOMs, defining the requirements for simulations that incorporate both mechanisms.

Table 1 summarises the parameters for the LHC ring, the main accelerating system, and the beam at injection, which were used as an input for the simulations. The parameters represent the baseline scenario for proton operation at injection into the HL-LHC [4].

Table 1: HL-LHC Accelerator, RF and Beam Parameters at Injection

Parameter	Unit	Value
Circumference, C	m	26 658.86
Harmonic number, h		35 640
Beam energy, E	GeV	450
Transition gamma, γ_{tr}		53.8
RF frequency, f_{RF}	MHz	400.788
RF voltage, V_0	MV	8
Bunch intensity, N_p	p/b	2.3×10^{11}

Both NB and BB impedances $Z(\omega)$ can be represented by a resonator model, described by an equivalent RCL circuit with a shunt impedance R_{sh} , a resonant angular frequency ω_r and a quality factor Q according to

$$Z(\omega) = \frac{R_{sh}}{1 + iQ \left(\frac{\omega}{\omega_r} - \frac{\omega_r}{\omega} \right)} \quad (1)$$

LOSS OF LANDAU DAMPING

To describe the BB part of the longitudinal impedance, a resonator with $Q = 1$, a cut-off frequency of $f_c = f_r = 5$ GHz and an effective imaginary impedance $(\text{Im}Z/k)_{\text{eff}} = 0.07 \Omega$ (LHC) or 0.075Ω (HL-LHC) is well suited [5]. Following Eq. 1, the shunt resistance can be expressed as $R_{sh} = (\text{Im}Z/k)_{\text{eff}} \times Q \times (f_r/f_{\text{rev}})$. The bunch shape is best described by a binomial distribution function, which, neglecting intensity effects, is given by the line density function

$$\lambda(t) = \lambda_0 \left(1 - \frac{\sin^2 \frac{\Delta t}{2}}{\sin^2 \frac{\tau_{\text{full}}}{2}} \right)^{\mu+0.5}, \quad (2)$$

with the binomial exponent μ , the normalisation constant λ_0 , Δt is the time coordinate with respect to the reference particle and τ_{full} the full bunch length. The bunches at injection in the LHC were observed to have an exponent

* Research supported by the HL-LHC project

[†] clara.charlotte.becker@cern.ch

$\mu = 1.5 - 2.0$, and the same value is assumed for the HL-LHC era.

The bunch shape and length have a considerable effect on the LLD threshold, since the threshold bunch intensity scales as [6]

$$N_{p,th} \propto \frac{\phi_{max}^5}{\mu(\mu + 1)\chi(y_{max}, \mu)}, \quad (3)$$

where the phase and bunch length are transformed by $\phi_{max} = \tau_{full}\omega_{rf}/2$, $y_{max} = k_{max}\phi_{max}/h$, with $k_{max} = f_c/f_{rev}$ and h being the harmonic number, $\chi(y, \mu) = y [1 - {}_2F_3(1/2, 1/2; 3/2, 2, \mu; -y^2)]$, where ${}_2F_3$ is the generalised hypergeometric function. The accurate resolution of the bunch halo is therefore essential, requiring sufficient macroparticles to avoid numerical errors that could effect the physical result. The simulations were set up with 64 bins per RF bucket and a resolution time span of four buckets. To evaluate the required number of macroparticles, a convergence study was performed. The bunch intensity and distribution were set to be slightly above the expected LLD threshold. After applying a 10° phase kick, oscillatory behaviour of the bunch was observed, indicating LLD. The bunch position oscillation amplitude was analysed for the last 2×10^4 , 3×10^4 and 5×10^4 turns of 9×10^4 simulated turns after the kick. For each number of macroparticles, the initial bunch distribution was generated with ten different seeds. Then, the mean of the bunch position oscillation amplitudes over the different seeds was evaluated and compared to the results for increasing numbers of macroparticles. The same set of simulations was performed at two different initial bunch lengths.

The study showed that, when increasing the number of macroparticles, the variation introduced by the seed is reduced and the value of the bunch position oscillation amplitude converged. The results are shown in Fig. 1. It was also found that, for cases where the bunch is highly unstable, fewer macroparticles are required to replicate the dynamics of the instability. Since the provided HL-LHC parameters are close to the threshold in most cases, and therefore probably not highly unstable, it was concluded that 10^7 macroparticles are needed for these single bunch simulations.

COUPLED-BUNCH INSTABILITIES

Two different types of crab cavities, the RF-Dipole (RFD) [7] and the Double-Quarter-Wave (DQW) [8] cavities will be installed for horizontal crabbing around the ATLAS experiment and for vertical crabbing around the CMS experiment, respectively. Each beam will traverse four cavities of each type. Calculations of CBI showed that, when neglecting the BB impedance, the HOM of the DQW crab cavity with $f_r = 582$ MHz, $R_{sh} = 73$ k Ω , and $Q = 1360$ leads to the lowest instability threshold [9]. Solely this mode was used for the discussed simulation and is represented as a single resonator impedance source. The worst case scenario was considered, where all four crab cavities have exactly the same resonant frequency, leading to a total $R_{sh, total} = 4 \times 73$ k $\Omega = 292$ k Ω .

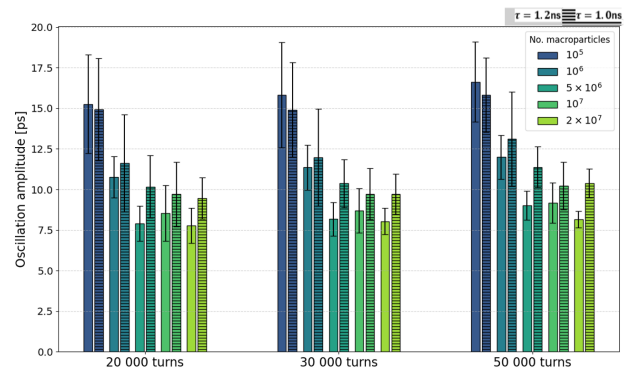


Figure 1: Oscillation amplitude of the bunch position observed in LLD simulations, averaged over ten simulations applying different seeds for the phase-space distribution. The colours represent different macroparticle numbers, while the full and dashed bars indicate different initial bunch lengths.

As in the LLD case, the initial step of the CBI analysis is to determine an adequate number of macroparticles for the simulations. For single-particle tracking, the computational complexity scales with the total number of macroparticles. To reduce the total number of macroparticles in the simulation, one should determine the minimum amount of bunches required to predict the behaviour of each bunch in a full ring. To investigate this, the decay of the wake field and the voltage induced by two trains of the so-called standard beam were analysed for the assumed resonator impedance. In the standard beam, each train consists of 4×72 bunches; the 72-bunch blocks will from now on be referred to as batch. An exemplary batch is indicated in Fig. 2 by the red box and a train by the black box. The bunches within each batch have a spacing of 25 ns. The distance between subsequent batches is 200 ns and the spacing between the two trains consisting of four batches is 800 ns. The number of macroparticles per bunch for all simulations in this analysis was chosen to be 10^5 . The line density of the bunches is again the binomial distribution function (Eq. 2), with a full bunch length of $\tau_{full} = 1.46$ ns and an exponent of $\mu = 1.5$.

Figure 3 illustrates the decay of the induced wake field during the gaps between bunches, batches, or trains. Figure 2 shows an example of the beam profile and its induced voltage. Counter-intuitively, the induced voltage does not build up with an increasing number of bunches. This can be explained by the interplay of the 40 MHz beam spectral lines and the HOM resonant frequency.

To analyse if the induced voltage experienced by the particles in the different batches and trains is similar, the growth rate of the instability of the last bunch of each batch for both trains was examined. It was noticed that with a bunch length of $\tau_{full} = 1.46$ ns and after 5×10^4 turns, an increase in the bunch position oscillation amplitude is visible. This could indicate that an instability starts to emerge, but more turns are needed to identify an instability growth rate. However, modelling a substantially larger amount of turns is difficult as the simulations are already runtime limited, even using GPU execution on the CERN computing cluster HTCCondor.

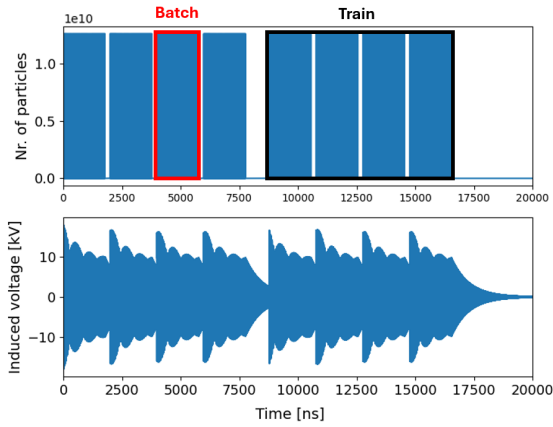


Figure 2: Beam profile for two trains of four 72 bunch batches (top). Resulting induced voltage (bottom) assuming a single NB resonator.

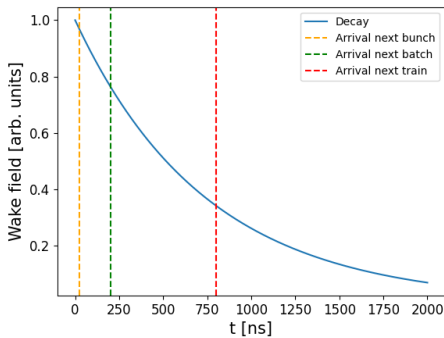


Figure 3: Decay of the wake field envelope for the NB resonator (blue). The vertical lines indicate the distance to the next bunch (yellow), batch (green), and bunch train (red).

Therefore, for a preliminary assessment, a shorter bunch length of $\tau_{\text{full}} = 0.67$ ns was used to artificially increase the growth rate of the instability.

Instabilities are characterised by exponential growth. The growth rate was analysed by fitting the logarithm of the upper envelope of the bunch position oscillation to a linear function, as illustrated in Fig. 4. The results are given in Table 2. With the exception of the first batches, the exponential growth of the bunch position emerges between turn 5000 and turn 9000. This was determined by identifying the turn interval yielding the best linear fit. The amplitude grows to about 0.35 ns. Notably, the growth rates for the respective batches are consistent across the different trains. Especially, for the third and fourth batch the evolution is almost identical in the analysed time frame. These observations suggest, that the presence of a second train mainly affects the first and second batch of the second train as the residual field of the first train is still present. The effect on the third and fourth batch appears to be negligible. This thereby indicates, that subsequent trains would probably behave similarly to the second one. For an analysis of the HOM impedance introduced by the crab cavities, it might therefore be sufficient to track only two trains.

Table 2: Simulated growth rate in units of 10^{-4} per turn. The asterisk indicates that the amplitude to which the bunch position grows is approximately a factor 0.1 smaller than for the rest of the bunches. For bunches number 72, the instability takes longer to develop than for the other bunches.

Bunch no.	72	144	216	288
$\tau_{\text{train1}}^{-1}$	4*	5	7	10
$\tau_{\text{train2}}^{-1}$	9	5	7	10

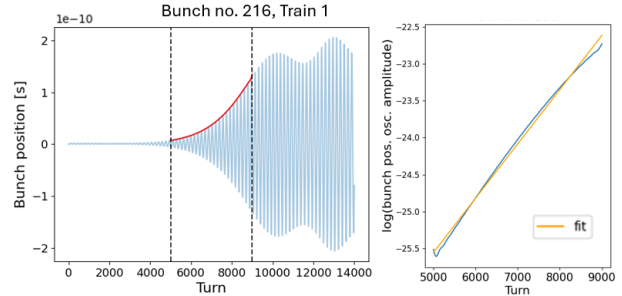


Figure 4: Example of a bunch position evolution with the envelope in red (left); the vertical lines indicate the region used for growth-rate analysis. Logarithm of the bunch position amplitude envelope with the linear fit in orange (right).

CONCLUSIONS AND OUTLOOK

For a thorough assessment of the longitudinal stability threshold at injection into the HL-LHC, both BB impedance and NB impedance effects need to be considered. The different computational needs for macroparticle simulations to investigate single-bunch effects caused by BB impedance, as well as coupled-bunch effects induced by NB impedance from the crab cavities, were discussed. Macroparticle convergence studies for simulating single-bunch LLD were performed and suggested that 10^7 macroparticles are required for the LHC case. With this amount of macroparticles per bunch, combined simulations of BB and NB effects cannot be simulated with the entire LHC beam (up to 2760 bunches) on the CERN computing clusters. To reduce the memory requirements and compute time, it was investigated if the number of bunches in the combined simulations could be reduced. To do so, pure NB simulations of the LHC beam with a low amount of macroparticles per bunch were performed. Based on the analysis on the induced voltage, the simulations suggest that it might be sufficient to perform the combined studies with a few trains only.

For the present studies, a short bunch length was set to reduce the run time of the simulations. In the future, the simulations shall be performed with more realistic bunch parameters. Furthermore, for a more complete description of the HL-LHC beam dynamics at injection, phase kicks due to the beam phase loop and the bunch length spread due to intra-beam scattering need to be included. Finally, simulations on the stability threshold at injection considering both instability effects shall be performed.

REFERENCES

- [1] I. Karpov and E. Shaposhnikova, “Generalized threshold of longitudinal multibunch instability in synchrotrons”, *Phys. Rev. Accel. Beams*, vol. 27, no. 7, p. 074401, Jul. 2024. doi:doi:10.1103/PhysRevAccelBeams.27.074401
- [2] I. Karpov *et al.*, “HL-LHC longitudinal beam stability for updated impedance model”, in *Proc. 15th HL-LHC Collaboration Meeting*, Sep. 2025. <https://indico.cern.ch/event/1559978/contributions/6664916/>
- [3] H. Timko *et al.*, “Beam longitudinal dynamics simulation studies”, *Phys. Rev. Accel. Beams*, vol. 26, no. 11, p. 114602, Nov. 2023. doi:10.1103/PhysRevAccelBeams.26.114602
- [4] R. Tomas Garcia *et al.*, “HL-LHC Run 4 proton operational scenario”, CERN, Geneva, Rep. CERN-ACC-2022-0001, 2022. <https://cds.cern.ch/record/2803611>
- [5] M. Zampetakis *et al.*, “Refining the LHC Longitudinal Impedance Model”, in *Proc. HB'23*, Geneva, Switzerland, Oct. 2023, pp. 559–562. doi:doi:10.18429/JACoW-HB2023-THBP37
- [6] I. Karpov, T. Argyropoulos, and E. Shaposhnikova, “Thresholds for loss of Landau damping in longitudinal plane”, *Phys. Rev. Accel. Beams*, vol. 24, no. 1, p. 011002, Jan. 2021. doi:10.1103/PhysRevAccelBeams.24.011002
- [7] S. U. DeSilva, P. Berrutti, J. R. Delaysen, N. A. Huque, and H. Park, “Room Temperature Measurements of Higher Order Modes for the SPS Prototype RF-Dipole Crabbing Cavity”, in *Proc. IPAC'18*, Vancouver, BC, Canada, Jun. 2018, pp. 3805–3807. doi:doi:10.18429/JACoW-IPAC2018-THPAL067
- [8] J. A. Mitchell, G. Burt, R. Calaga, S. Verdú-Andrés, and B. P. Xiao, “DQW HOM Coupler Design for the HL-LHC”, in *Proc. IPAC'18*, Vancouver, BC, Canada, Jun. 2018, pp. 3663–3666. doi:doi:10.18429/JACoW-IPAC2018-THPAL018
- [9] I. Karpov and E. Shaposhnikova, “Impact of Broadband Impedance on Longitudinal Coupled-Bunch Instability Threshold”, in *Proc. IPAC'22*, Bangkok, Thailand, Jun. 2022, pp. 2245–2248. doi:10.18429/JACoW-IPAC2022-WEPOMS008